

Scattering and absorption of terahertz waves by a free-standing infinite grating of graphene strips: analytical regularization analysis

This content has been downloaded from IOPscience. Please scroll down to see the full text.

2015 J. Opt. 17 055604

(<http://iopscience.iop.org/2040-8986/17/5/055604>)

View [the table of contents for this issue](#), or go to the [journal homepage](#) for more

Download details:

IP Address: 169.230.243.252

This content was downloaded on 19/04/2015 at 00:21

Please note that [terms and conditions apply](#).

Scattering and absorption of terahertz waves by a free-standing infinite grating of graphene strips: analytical regularization analysis

Tatiana L Zinenko

Institute of Radio-Physics and Electronics NASU, Proskury st. 12, 61085 Kharkiv, Ukraine

E-mail: tzinenko@yahoo.com

Received 14 November 2014, revised 16 February 2015

Accepted for publication 9 March 2015

Published 17 April 2015



CrossMark

Abstract

The plane wave scattering and absorption by an infinite flat graphene strip grating in the free space are studied in the THz range in the H- and E-polarization regimes. Accurate numerical treatment is based on the dual series equations and the analytical regularization technique. The resulting numerical algorithm possesses guaranteed convergence and controlled accuracy of computations. Reflectance, transmittance and absorbance by the graphene-strip gratings are studied as a function of various parameters. In the H-polarization case, the dominant feature is the excitation of the surface plasmon resonances on each strip. In the E-polarization case, Rayleigh anomalies are the only observable features.

Keywords: graphene strip grating, scattering, absorption, analytical regularization, dual series

1. Introduction

This paper presents a mathematically grounded study of the absorption and scattering of THz waves by a flat graphene-strip grating in free space (see figure 1). Such suspended-graphene structures, although less usual than substrate-on configurations, are also under study today [1, 2]. In addition, such an analysis enables one to see clearly what features in the scattering and absorption are characteristic to the grating itself that can be useful when comparing them to the more complicated effects observed for the substrate-on gratings.

Graphene is a single-atom layer which displays good electron conductivity that depends on frequency, temperature, electron relaxation time and chemical doping [3]. Thus, it can be simulated as a zero-thickness imperfect and partially transparent conductor, i.e. an electrically resistive sheet characterized with frequency-dependent complex valued resistivity. Graphene is also famous for its strong interaction with electromagnetic waves of the THz frequency range [4–13]. Thanks to the properties of its conductivity a sheet of graphene is able to support delocalized surface plasmon waves at frequencies two orders of magnitude lower than the

noble metals. Compared to metals, the most interesting for the applications feature of graphene is the opportunity to modify its conductivity by applying an external electrostatic biasing field, which modifies graphene chemical potential. In practice, this can be arranged by including a thin metal or semiconductor layer below the dielectric substrate, which supports graphene, and by applying a DC bias between two layers.

Patterned graphene offers more degrees of freedom in manipulation with THz waves. Its prospective applications are multiple and include fixed and reconfigurable periodic frequency selective surfaces, plasmonic waveguides, tunable switches, infrared and THz sensors, antennas and absorbers [4–11]. Here, the periodic arrays of graphene strips have already attracted the attention of researchers as easily manufactured frequency-selective surfaces and efficient absorbers in the THz frequency range. Their analysis meets the same difficulties as for the resistive-strip gratings at microwaves in which the resistivity has been usually assumed to be a real-valued constant [14–17].

The wave scattering and absorption by an infinite grating of coplanar graphene strips have been analyzed using the Fourier expansion method [6, 10] and commercial solvers

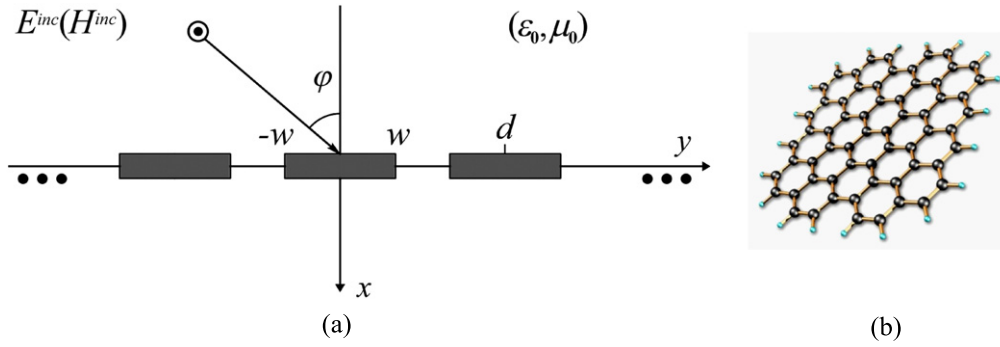


Figure 1. Cross-sectional geometry of a graphene-strip grating scattering problem (a) and a close view of the graphene layer (b).

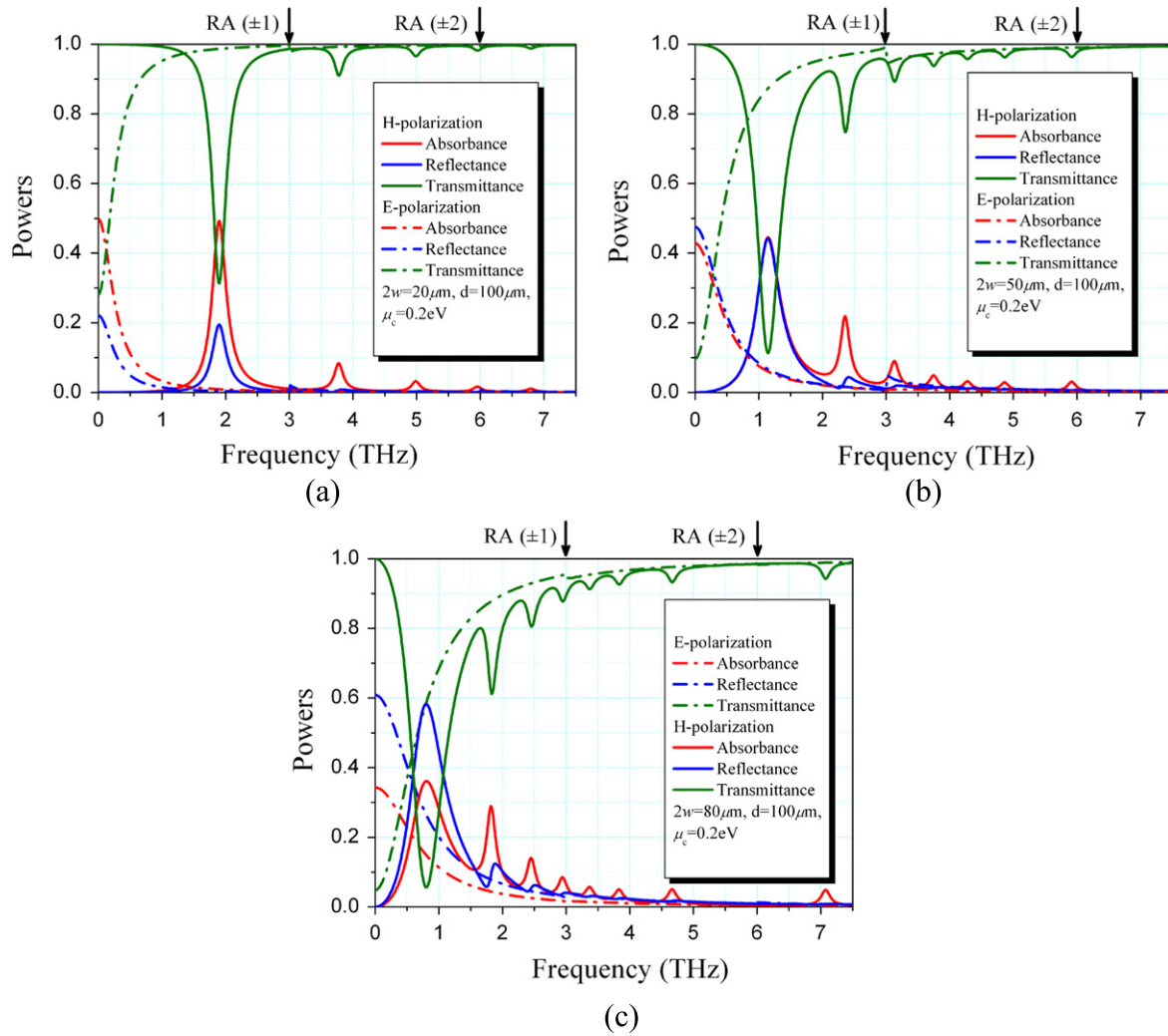


Figure 2. The spectra of the power fractions of transmittance, reflectance and absorbance for the graphene-strip grating with the period $d = 100 \mu\text{m}$ under the normal incidence ($\varphi = 0^\circ$) of the H-polarized (solid curves) and the E-polarized (dashed curves) plane wave. The strip widths are $2w = 20 \mu\text{m}$ (a), $50 \mu\text{m}$ (b) and $80 \mu\text{m}$ (c).

such as Comsol [7–10], and the plasmon-assisted resonances in the H-polarized plane have been reported.

Unfortunately, while able to reveal basic physical effects, the Fourier method does not lead to a convergent numerical algorithm in the case of H-polarization scattering by a resistive strip grating. Indeed, as noted in [17], inspection of the elements of the matrix equations derived in [14] and [16]

shows that they do not decrease with larger indices and therefore are not able to yield a convergent solution for progressively larger values of the order of truncation. Practically speaking, this means that although a few digits in the solution can be found correctly, the algorithm fails to yield the results with better accuracy. Note further that the accuracy of numerical solutions obtained with commercial solvers cannot

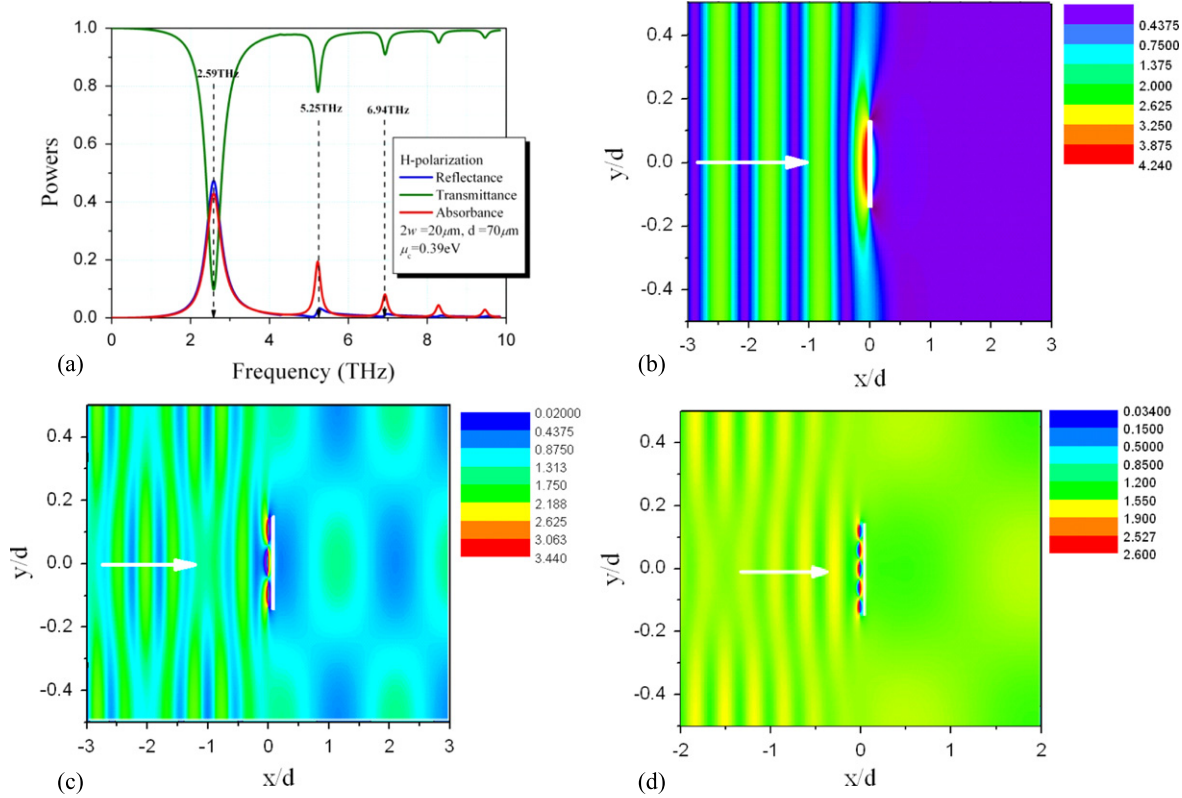


Figure 3. (a) Reflectance, transmittance and absorbance as a function of the frequency for the scattering of the H-wave from the grating of narrow graphene strips. $\varphi = 0^\circ$, $2w = 20 \mu\text{m}$ and $d = 70 \mu\text{m}$. The graphene parameters are $\tau = 1 \text{ ps}$, $\mu_c = 0.39 \text{ eV}$ and $T = 300 \text{ K}$. (b)–(d) The magnetic field patterns on the elementary period in the surface-plasmon resonances P_1 at $f = 2.59 \text{ THz}$, P_3 at $f = 5.25 \text{ THz}$ and P_5 at $f = 6.94 \text{ THz}$, marked with dotted lines in (a).

be controlled by users. Any solver is advertised as accurate and convergent however remains a ‘black box’ whose internal structure and underlining mathematics is known to developers only.

In contrast, in [11] the scattering by finite and infinite graphene strip gratings has been treated using the singular integral equations and Nystrom-type quadrature formulas for their discretization. The convergence of this approach is guaranteed by the mathematical theorems about the approximation of integrals by quadratures. This has enabled accurate quantification of properties of the graphene-strip gratings, including plasmon resonances. We have used the results of [11] as a reference; as both methods generate convergent numerical algorithms, we could see a coincidence in the obtained data within an arbitrary number of digits, controlled by the order of discretization.

Our approach to the electromagnetic analysis of graphene-strip gratings uses the method of dual series equations and analytical regularization developed in [17, 18] and supplemented with the model of graphene conductivity of [3]. This latter model is based on the Kubo formula and leads to the frequency-dependent resistivity, also called surface impedance, in view of its complex value. Regularization can be alternatively achieved by using the singular integral equation and its projection to certain polynomials, as in [19]. The convergence of the algorithm developed on this basis is guaranteed by the Fredholm theorems because the resulting matrix equations are of the Fredholm second kind. Then, the

accuracy of the solution is easily controlled by the matrix truncation order. Another attractive feature is that the accuracy does not depend on the relation between the size of the strip and the period of the grating. Finally, the conservation of power is kept at the level of machine precision for arbitrary frequency and grating parameters.

2. Problem statement and basic equations

Consider the 2D scattering of a time-harmonic plane wave by a grating made of graphene strips, as is illustrated in figure 1. Assume that the time dependence is given as $e^{+j\omega t}$. An infinite number of zero-thickness conducting strips, parallel to the z -axis, is located in the plane $x = 0$ with period d . Each strip has the width $2w$. The propagation vector of the incident plane wave makes the angle φ with respect to the negative x -axis. The field, scattered by the grating, should satisfy the Helmholtz equation and the boundary conditions that couple the tangential field components on the strip surface

$$\begin{aligned} & \frac{1}{2} \left[\vec{E}_T^+(x, y) + \vec{E}_T^-(x, y) \right] \\ & = R \vec{x} \times \left[\vec{H}_T^+(x, y) - \vec{H}_T^-(x, y) \right], \\ & \vec{E}_T^+(x, y) = \vec{E}_T^-(x, y), \\ & x = 0, |y - nd| < w, n = \pm 1, \pm 2, \dots \end{aligned} \quad (1)$$

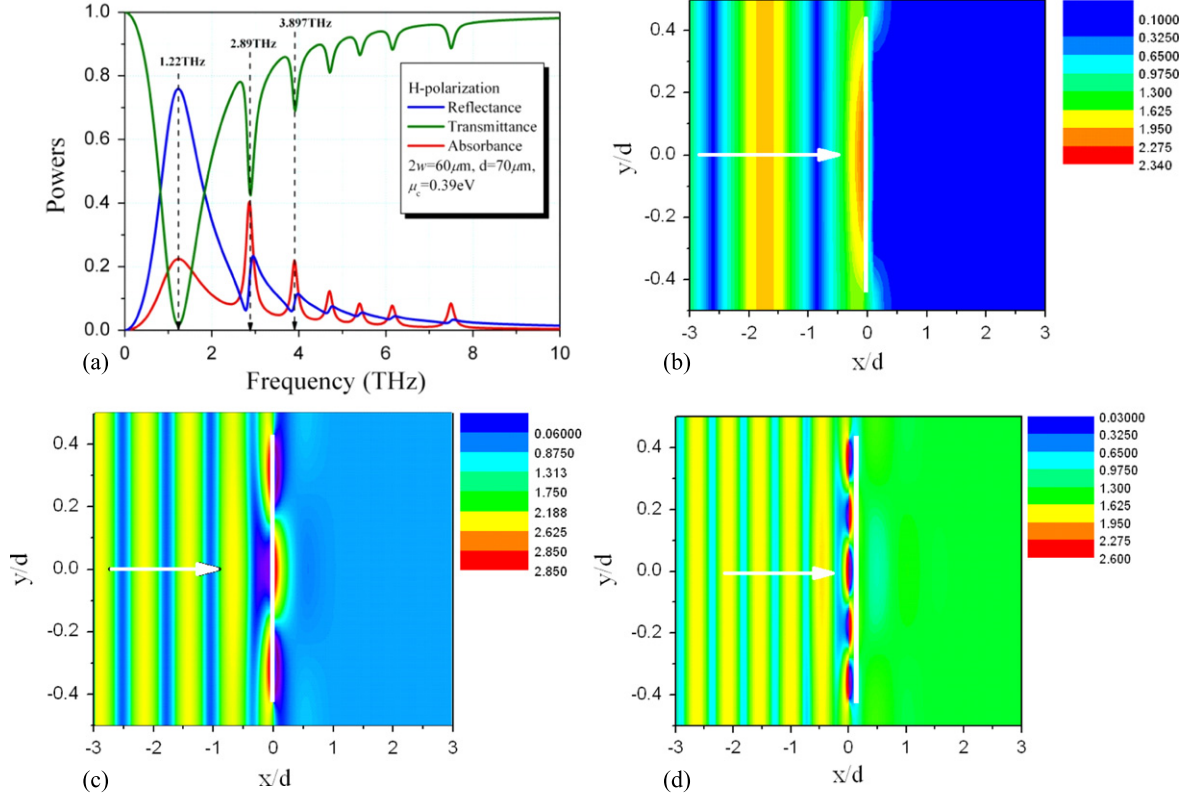


Figure 4. (a) Reflectance, transmittance and absorbance as a function of the frequency for the scattering of the H-wave from the grating of wide graphene strips. $\varphi = 0^\circ$, $2w = 60 \mu\text{m}$ and $d = 70 \mu\text{m}$. The graphene parameters are $\tau = 1 \text{ ps}$, $\mu_c = 0.39 \text{ eV}$ and $T = 300 \text{ K}$. (b)–(d) The magnetic field patterns on the elementary period in the surface-plasmon resonances P_1 at $f = 1.22 \text{ THz}$, P_3 at $f = 2.89 \text{ THz}$ and P_5 at $f = 3.897 \text{ THz}$, marked with dotted lines in (a).

Here, $R = 1/\sigma$, σ is the graphene surface electron conductivity, the superscript \pm indicates the limiting value of the function at $x \rightarrow \pm 0$, the subscript T components tangential to the strips and \vec{x} is the unit normal vector.

For the uniqueness of the solution, we complete the formulation, similarly to [17–19], with the edge condition and the radiation condition at $x \rightarrow \pm\infty$. The latter condition demands that the field power contained in any finite domain, including a strip edge, is bounded [20]. The former requests that the field is expandable in terms of convergent series of the outgoing (finite number) and exponentially decaying (infinite number) Floquet–Rayleigh spatial harmonics (i.e. diffraction orders).

The scattering problem consists of the finding of the z -component (i.e. E_z or H_z , depending on polarization) of the total electromagnetic field, $U = U^{inc} + U^{sc}$. The incident field function corresponding to the plane wave incident at the angle φ to the x -axis is given by $U^{inc} = e^{-jk_0(x \cos \varphi + y \sin \varphi)}$. The grating periodicity along the y -axis assures a quasi-periodicity of the total field $U(x, y + d) = U(x, y)$. Due to this fact the scattered field can be expanded in terms of the Floquet series like

$$\begin{cases} E_z^{sc}(x, y) \\ H_z^{sc}(x, y) \end{cases} = \sum_{n=-\infty}^{\infty} \begin{cases} a_n, & x > 0 \\ b_n, & x < 0 \end{cases} e^{-j(a_n|x| + \beta_n y)}, \quad (2)$$

where a_n and b_n are the amplitudes of the Floquet harmonics in transmission and reflection half-space, respectively, $\alpha_n = (k_0^2 - \beta_n^2)^{1/2}$ and $\beta_n = \beta_0 + 2\pi n/d$ are the propagation constants of the spatial harmonics of the n th order, $k_0 = \omega/c$ and ω is the cyclic frequency. In addition, in the case considered in this paper, the radiation condition requires that for each mode, either $\text{Re } \alpha_{n>0} \geq 0$ or $\text{Im } \alpha_n \leq 0$, owing to the $e^{+j\omega t}$ time dependence.

Consider first the H -polarized wave case, where $\vec{H}_T = H_z \vec{z}_0$, $\vec{E}_T = E_y \vec{y}_0$, and $E_y = (j\zeta_0/k_0)\partial H_z/\partial x$. The amplitudes a_n and b_n are coupled by the boundary conditions (1) on the strip and the continuity conditions across the slot domain. Hence, the equation $E_T^+(x, y) = E_T^-(x, y)$ is valid for all y and $x = 0$. This yields $b_n = -a_n$, so one set of coefficients, say, b_n , can be excluded from further consideration.

To determine the coefficients a_n we use the dual set of boundary conditions that hold on complimentary subintervals of strip (M) and slot (S) on the elementary period, namely

$$\begin{aligned} \frac{1}{2}(E_y^+ + E_y^-) &= R(H_z^- - H_z^+), & (x, y) \in M \\ H_z^+ &= H_z^-, & (x, y) \in S. \end{aligned} \quad (3)$$

By introducing the notations $\varphi = -2\pi y/d$, $\theta = 2\pi w/d$, $g_n = [1 - (\sin \phi + n/\kappa)^2]^{1/2}$, $r_n = |n| - j\kappa g_n$ and using the

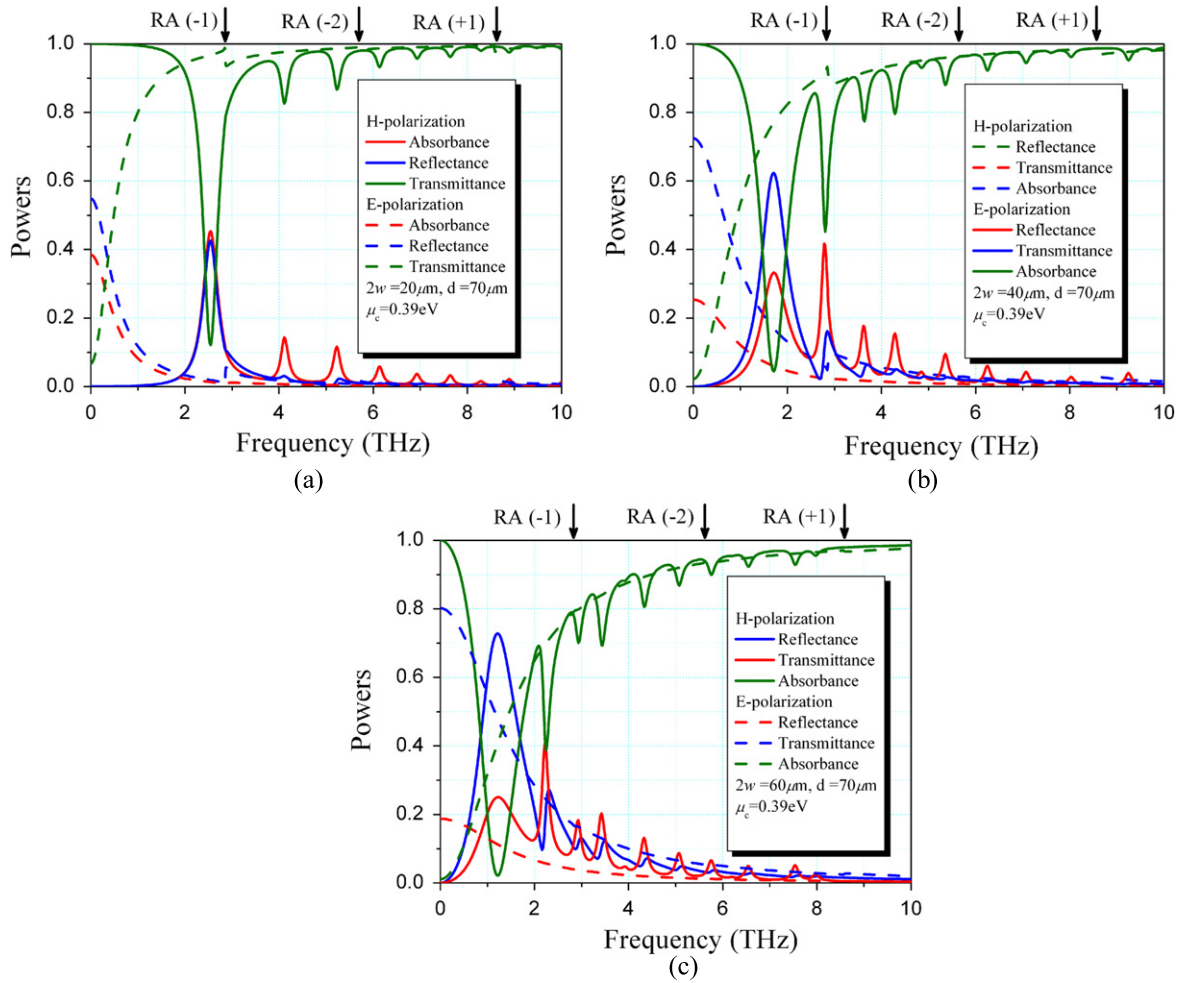


Figure 5. The spectra of the power fractions of transmittance, reflectance and absorbance for the graphene-strip grating with the period $d = 70 \mu\text{m}$ under the oblique incidence ($\varphi = 30^\circ$) of the H-polarized (solid curves) and the E-polarized (dashed curves) plane wave. The strip widths are $2w = 20 \mu\text{m}$ (a), $40 \mu\text{m}$ (b) and $60 \mu\text{m}$ (c). The graphene parameters are $\tau = 1 \text{ ps}$, $\mu_c = 0.39 \text{ eV}$ and $T = 300 \text{ K}$.

series (2), we arrive at the dual series equations (DSEs)

$$\begin{cases} \sum_{n=-\infty}^{\infty} a_n |n| e^{jn\phi} = r_0 + \sum_{n=-\infty}^{\infty} a_n (r_n - 2j\kappa R / \zeta_0) e^{jn\phi}, & |\phi| < \theta \\ \sum_{n=-\infty}^{\infty} a_n e^{jn\phi} = 0, & \theta < |\phi| \leq \pi, \end{cases} \quad (4)$$

where $\zeta_0 = (\mu_0/\epsilon_0)^{1/2}$ is the free space impedance. It should be noted that $r_0 = O(\kappa)$, $r_n = \kappa O(1 + \kappa/|n|)$, $g_0 = O(1)$ and $g_{n \neq 0} = O(|n/\kappa|)$ at $\kappa|n|^{-1} \rightarrow 0$. Owing to this fact the singular (static) part of the DSE operator (i.e. the part corresponding to $k_0 d \rightarrow 0$) can be inverted using the Riemann–Hilbert problem (RHP) technique. The exact analytical solution to the RHP, as given in [21], yields an infinite system of linear algebraic equations. In operator form it can be presented as follows:

$$(I + A^H)X = B^H, \quad (5)$$

where

$$\begin{aligned} X &= \{a_n\}_{n=-\infty}^{\infty}, \\ A &= \{A_{mn}^H\}_{m,n=-\infty}^{\infty}, \\ A_{mn}^H &= (2j\kappa R / \zeta_0 - r_n) T_{mn}(\theta) \\ I &= \{\delta_{mn}\}_{m,n=-\infty}^{\infty}, \\ B &= \{B_m^H\}_{m=-\infty}^{\infty}, \\ B_m^H &= r_0 T_{m0}(\theta), \end{aligned}$$

and coefficients $T_{mn}(\theta)$ are the combinations of Legendre polynomials and can be found in [15, 19]. Using the large-index asymptotics of these polynomials, one can verify that $T_{mn}(\theta) = O(|mn|^{-1/2} |m - n + 1|^{-1})$ for all θ . This allows one to prove that the L_2 operator norm $\|A\|^2 < \infty$ and hence (5) is a regularized matrix equation, i.e. of the Fredholm second kind. It can also be shown that the solution based on (5) satisfies the edge condition. This is due to the fact that the edge behavior is taken into account explicitly when inverting

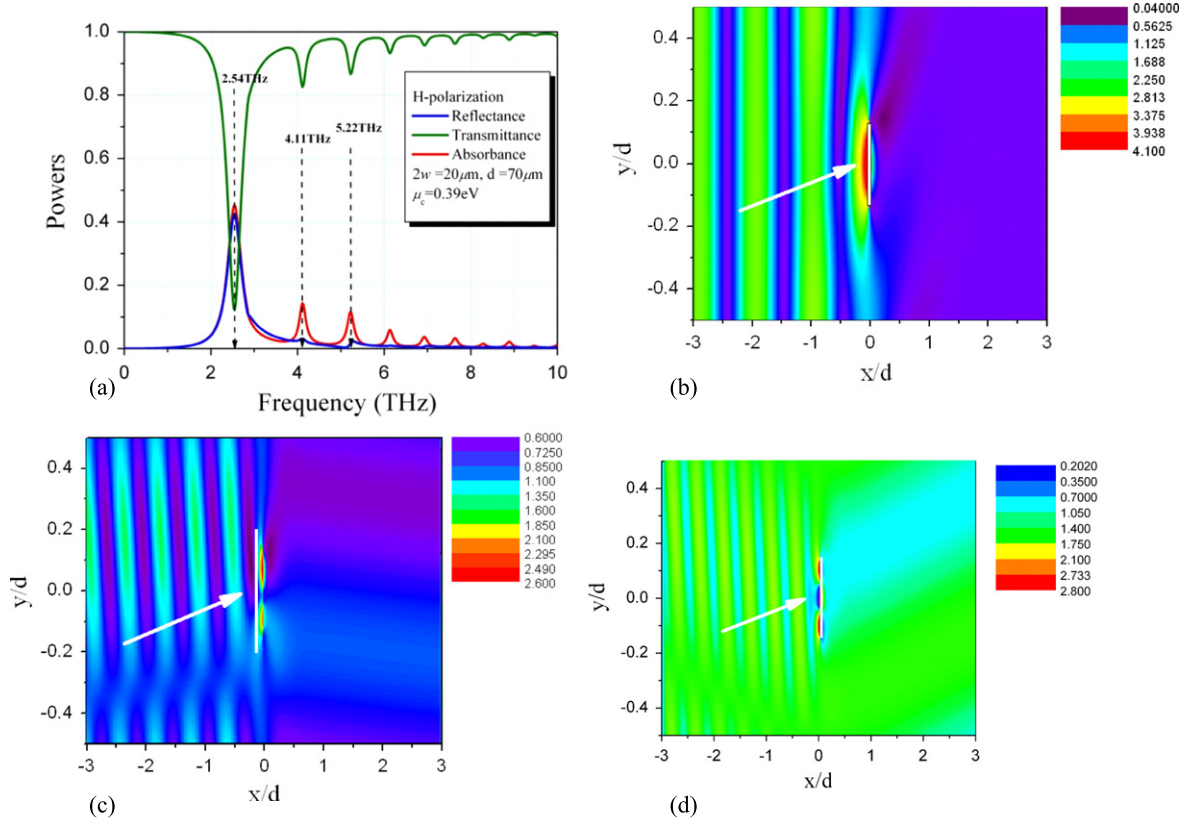


Figure 6. (a) Reflectance, transmittance and absorbance as a function of the frequency for the scattering of the H-wave from the grating of graphene strips. $\varphi = 30^\circ$, $2w = 20 \mu\text{m}$, $d = 70 \mu\text{m}$. The graphene parameters are $\tau = 1 \text{ ps}$, $\mu_c = 0.39 \text{ eV}$ and $T = 300 \text{ K}$. (b)–(d) The graphene parameters are $\tau = 1 \text{ ps}$, $\mu_c = 0.39 \text{ eV}$ and $T = 300 \text{ K}$. (b)–(d) The magnetic field patterns on the elementary period in the surface-plasmon resonances P_1 at $f = 2.54 \text{ THz}$, P_2 at $f = 4.11 \text{ THz}$ and P_3 at $f = 5.22 \text{ THz}$, marked with dotted lines in (a).

the RHP [21]. Note that to arrive at (5), we have avoided the meshing of the strip and have not used numerical integration to fill in the matrix. Additionally, since at $\kappa = 0$ all matrix elements equal zero, (5) yields the exact analytical solution in the static case.

The Fredholm nature of the matrix equation (5) justifies the truncation to finite order when solving it numerically because solutions obtained with progressively larger orders of truncation lead to smaller errors. Thus, the convergence, in mathematical sense, is guaranteed. Note that the matrix elements and the right-hand part elements are the combinations of elementary functions and can be easily computed to machine precision. Then, the accuracy of the numerical solution is controlled by the order of truncation. In addition, for the Fredholm second-kind matrices, the condition numbers (i.e. the product of the norm of the matrix and the norm of the inverse matrix) are finite and usually quite moderate. In other words, equation (5) is well conditioned for an arbitrary set of the problem parameters.

This is in contrast to the Fourier-expansion method and its derivatives used in papers [6, 14, 15] in which convergence is absent and as a result the accuracy is limited to a few first digits.

Consider now the E-polarized wave case. Then, $\vec{E}_T = E_z \vec{z}_0$, $\vec{H}_T = H_y \vec{z}_0$, and $H_y = (1/jk_0)\partial E_z/\partial x$. Instead of (3) we have now the dual conditions

$$\begin{aligned} \frac{1}{2}(E_z^+ + E_z^-) &= R(H_y^+ - H_y^-), (x, y) \in M \\ H_y^+ &= H_y^-, (x, y) \in S. \end{aligned} \quad (6)$$

From the continuity of electric field tangential components on the strip, it follows that $a_n = b_n$ in this polarization. By using conditions (6), we obtain a series equation as follows:

$$\sum_{n=-\infty}^{\infty} a_n g_n e^{jn\phi} = \begin{cases} -\frac{1}{2R/\zeta_0} \left(1 + \sum_{n=-\infty}^{\infty} a_n e^{jn\phi} \right), & |\phi| < \theta \\ 0, & \theta < |\phi| \leq \pi \end{cases} \quad (7)$$

The left-hand side of (7) can be inverted analytically by using inverse Fourier transform and the orthogonality of the exponents. This leads to the following set of equations:

$$a_m = \frac{-1}{2R/\zeta_0 g_m} \sum_{n=-\infty}^{\infty} a_n S_{mn}(\theta) - \frac{S_{m0}(\theta)}{2R/\zeta_0 g_m}, \quad (8)$$

where $m = 0, \pm 1, \pm 2, \dots$ and the functions $S_{mn}(\theta)$ are

$$S_{mn}(\theta) = \frac{\sin(n-m)\theta}{(n-m)\pi}, \quad S_{mm}(\theta) = \frac{\theta}{\pi}. \quad (9)$$

Further, note that the rate of decay of the matrix elements of (8) with respect to the large $|n|$ and large $|m|$ is different. To symmetrize it, we introduce new variables, $x_n = a_n w_n$ with the weight $w_n = (|n| + 1)^{1/2}$ and arrive at the matrix equation

$$(I + A^E)X = B^E, \quad (10)$$

where

$$A = \left\{ A_{mn}^E \right\}_{m,n=-\infty}^{\infty}, \quad A_{mn}^E = \frac{S_{mn}(\theta)}{2R/\zeta_0} \frac{w_m}{g_m w_n},$$

$$X = \{x_n\}_{n=-\infty}^{\infty}, \quad I = \{\delta_{mn}\}_{m,n=-\infty}^{\infty}$$

$$B = \left\{ B_m^E \right\}_{m=-\infty}^{\infty}, \quad B_m^E = -\frac{S_{m0}(\theta)}{2R/\zeta_0} \frac{w_m}{g_m}.$$

Here, $\|A^E\| < \infty$ in L_2 for any $R \neq 0$, since for large $|m|$ $A_{mn}^E = O(|mn|^{-1/2}|m-n+1|^{-1})$. Hence, (10) is an operator equation of the Fredholm second kind. One can show that the field and current components built after solving (10) satisfy the edge condition. Note that no meshing of the strip is used, and no numerical integration is needed to fill in the matrix. Additionally, at $\kappa = 0$ all matrix elements equal zero except A_{0n}^E that allows one to obtain the static problem analytical solution.

3. Numerical results

Turning to numerical results, we present in figures 2 to 4 the frequency dependences of the power fractions of transmittance (T), reflectance (R) and absorbance (A) for three gratings illuminated by the normally incident H- and E-polarized plane waves of unit amplitude. Similar results are also shown for the oblique incidence in figures 5 and 6. Note that they satisfy the power conservation equation $T + R + A = 1$ at the level of machine precision.

In the computations, we have used the Kubo formula for characterization of the complex-valued electron conductivity of the graphene monolayer [3]. In addition, we took the strip width well above the 100 nm value that is considered as a limit for the use of Kubo formalism, as according to [22], the conductivity of narrower strips starts depending on the edge effects. The truncation orders of the matrix equations (5) and (10) have been adapted accordingly to the formula $N = \kappa(1 + |R|^{\pm 1/2}) + 10$ in the H-case and E-case, respectively, to provide 4-digit accuracy, even in the high-frequency part of the studied range.

In the case of the H-polarization, one can see a sequence of resonances on the surface-plasmon modes excited on every strip. Each of these modes can be interpreted as a Fabry–Perot standing wave formed by the reflections of the surface-plasmon natural wave of a graphene monolayer from the strip edges [23] (note a misprint in equation (14) of [23]). The complex propagation constant of this wave can be found

analytically using the conditions (1), which yield

$$\gamma_{pl} = k_0 \left[1 - (2R/\zeta_0)^2 \right]^{1/2} = k_0 \left[1 - (2/\sigma \zeta_0)^2 \right]^{1/2}. \quad (11)$$

Neglecting the losses and assuming a zero reflection phase of such a wave from the strip edge, the resonance frequencies can be found as roots of approximate characteristic equations, of which the common form is

$$\sin(\text{Re} \gamma_{pl} w) \approx 0, \quad (12)$$

which yields $\text{Re} \gamma_{pl} w \approx s\pi$, $s = 1, 2, 3, \dots$. Here, the roots, i.e. the natural frequencies of the odd and even with respect to the strip center modes, correspond to the odd ($s = 1, 3, \dots$) or even ($s = 2, 4, \dots$) values of the index, respectively. Note that in the case of the normal incidence (figures 2 to 4) only the odd-index surface-plasmon resonances are excited because of their modal field symmetry across the strip center; the even-index resonances need inclined incidence.

In the E-polarization case, the frequency dependences of the transmittance, reflectance and absorbance are much smoother than in the H-case as the surface-plasmon natural modes are absent. This is because the corresponding infinite sheet of graphene cannot support surface-plasmon waves in the E-polarization, i.e. with the electric field parallel to the sheet. The only visible features are the ± 1 -st and the ± 2 -d Rayleigh anomalies at 3 THz and 6 THz, respectively, denoted in figure 2, where the period of 100 μm is a multiple to the wavelength.

As one can see from the plots in figures 2 to 6, the position of the first plasmon resonance depends on the strip width. At the frequencies lower than this resonance, say, below 0.5 THz (exact value depends of the graphene chemical potential and other parameters), the graphene-strip grating displays the discrimination of polarizations: the H-polarized wave is well transmitted, while the E-polarized wave is well reflected. This property can be used in the design of tunable frequency filters or direction-of-arrival filters.

In figures 3(b) to (d), we show the magnetic near-field patterns in the surface-plasmon resonances: P_1 at $f = 2.59$ THz, P_3 at $f = 5.25$ THz and P_5 at $f = 6.94$ THz, marked in figure 3, on the elementary period of the grating for the scattering of the normally incident H-polarized wave. As mentioned above, in the case of the normal incidence, only the odd-index surface-plasmon resonances are excited. The even-index surface-plasmon resonances are not excited because of the orthogonal symmetry of their modal fields relative to the incident-field symmetry.

Figures 4(b) to (d) demonstrate the features of the surface-plasmon resonances on a graphene-strip grating with strips three times wider than those in figure 3. The near-zone patterns of the absolute value of the magnetic field correspond to the surface-plasmon resonances P_1 at $f = 1.22$ THz, P_3 at $f = 2.89$ THz and P_5 at $f = 3.897$ THz.

Figure 5 shows the spectra of the power fractions of transmittance, reflectance and absorbance for a graphene-strip grating under the oblique incidence ($\varphi = 30^\circ$) of the H-polarized (solid curves) and the E-polarized (dashed curves)

plane wave. The number of resonances in comparison with the case of normal incidence (figure 2) increases since both the odd-index and the even-index surface-plasmon resonances are now excited. This observation is supported by the magnetic field patterns in the resonances P_1 at $f=2.54$ THz, P_2 at $f=4.11$ THz and P_3 at $f=5.22$ THz, shown in figures 6(b) to (d). The direction of propagation of the incident plane wave is shown by the white arrow.

4. Conclusions

We have presented the dual-series equation technique supplemented with the analytical regularization procedure in the accurate numerical analysis of the scattering and absorption of THz waves by a free-standing infinite grating of graphene strips. Both the E- and H-polarization cases have been considered. The resulting meshless numerical solution does not involve any numerical integrations, has accuracy controlled by the size of the matrix equation and possesses guaranteed convergence that can be brought to machine precision.

Using this accurate computational instrument, we have quantified the surface-plasmon resonances observed in the H-polarization and have revealed less-pronounced variations of transmittance, reflectance and absorbance in the E-polarization at the Rayleigh anomalies. These results can be potentially useful in the computer-aided design and optimization of the filtering components on the basis of periodically patterned graphene. They can also be used in the verification of less accurate however more versatile numerical codes and commercial software.

Extension of the analysis to the substrate-supported graphene-strip gratings and to multi-layered gratings is straightforward and will be a subject of separate publications.

Acknowledgments

This work has been supported in part by the National Academy of Sciences of Ukraine via the State Target program ‘Nanotechnologies and Nanomaterials,’ project no. 1.1.3.45. The author is grateful to O V Shapoval, A I Nosich and M V Balaban for their fruitful discussions.

References

- [1] Du X, Skachko I, Barker A and Andrei E Y 2008 Approaching ballistic transport in suspended graphene *Nat. Immunology* **3** 491–5
- [2] Low T and Avouris P 2014 Graphene plasmonics for terahertz to mid-infrared applications *ACS Nano* **8** 1086–101
- [3] Gusynin V P, Sharapov S G and Carbotte J P 2007 Magneto-optical conductivity in graphene *J. Phys.: Condens. Matter* **19** 026222
- [4] Christensen J, Manjavacas A, Thongrattanasiri S, Koppens F H L and Garcia de Abajo F J 2012 Graphene plasmon waveguiding and hybridization in individual and paired nanoribbons *ACS Nano* **6** 431–40
- [5] Filter R, Farhat M, Steglich M, Alaei R, Rockstuhl C and Lederer F 2013 Tunable graphene antennas for selective enhancement of THz emission *Opt. Exp.* **21** 3737–45
- [6] Nikitin A Y, Guinea F, Garcia-Vidal F J and Martin-Moreno L 2012 Surface plasmon enhanced absorption and suppressed transmission in periodic arrays of graphene ribbons *Phys. Rev. B* **85** 081405(R)/4
- [7] Thongrattanasiri S, Koppens F H L and Garcia de Abajo F J 2012 Complete optical absorption in periodically patterned graphene *Phys. Rev. Lett.* **108** 047401–5
- [8] Vasic B, Isic G and Gajic R 2013 Localized surface plasmon resonances in graphene ribbon arrays for sensing of dielectric environment at infrared frequencies *J. Appl. Phys.* **113** 113110/7
- [9] Li K, Ma X, Zhang Z, Xu Y and Song G 2014 Tunable and angle-insensitive plasmon resonances in graphene ribbon arrays with multispectral diffraction response *J. Appl. Phys.* **115** 104306/6
- [10] Hwang R-B 2014 Rigorous formulation of the scattering of plane waves by 2D graphene-based gratings: out-of-plane incidence *IEEE Trans. Antennas Propag.* **62** 4736–45
- [11] Shapoval O V, Gomez-Diaz J S, Perruisseau-Carrier J, Mosig J and Nosich A I 2013 Integral equation analysis of plane wave scattering by coplanar graphene-strip gratings in the THz range *IEEE Trans. Terahertz Sci. Techn.* **3** 666–73
- [12] He X and Lu H 2014 Graphene-supported tunable extraordinary transmission *Nanotechnology* **25** 325201
- [13] He X 2015 Tunable terahertz graphene metamaterials *Carbon* **82** 229–37
- [14] Hall R C and Mittra R 1985 Scattering from a periodic array of resistive strips *IEEE Trans. Antennas Propag.* **AP-33** 1009–11
- [15] Petit R and Tayeb G 1990 Theoretical and numerical study of gratings consisting of periodic arrays of thin and lossy strips *J. Opt. Soc. Amer.* **7A** 1686–92
- [16] Volakis J L, Lin Y C and Anastassiou H 1994 TE characterization of resistive strip gratings on a dielectric slab using a single-mode expansion *IEEE Trans. Antennas Propag.* **42** 205–13
- [17] Zinenko T L, Nosich A I and Okuno Y 1998 Plane wave scattering and absorption by resistive-strip and dielectric-strip periodic gratings *IEEE Trans. Antennas Propag.* **46** 1498–505
- [18] Zinenko T L and Nosich A I 2006 Plane wave scattering and absorption by flat gratings of impedance strips *IEEE Trans. Antennas Propag.* **54** 2088–95
- [19] Matsushima A, Zinenko T L, Nishimori H and Okuno Y 2000 Plane wave scattering from perpendicularly crossed multilayered strip gratings *Prog. Electromagn. Res.* **28** 189–207
- [20] Braver I M, Fridberg P S, Garb K L and Yakover I M 1988 The behavior of the electromagnetic field near the edge of a resistive half-plane *IEEE Trans. Antennas Propag.* **36** 1760–8
- [21] Nosich A I 1993 Green’s function—dual series approach in wave scattering from combined resonant scatterers *Analytical and Numerical Methods in Electromagnetic Wave Theory* ed M Hashimoto, M Idemen and O A Tretyakov (Tokyo: Science House) pp 419–69
- [22] Han M Y, Oezylmaz B, Zhang Y and Kim P 2007 Energy band gap engineering of graphene nanoribbons *Phys. Rev. Lett.* **98** 206805
- [23] Balaban M V, Shapoval O V and Nosich A I 2013 THz wave scattering by a graphene strip and a disk in the free space: integral equation analysis and surface plasmon resonances *IOP J. Optics* **15** 4007–16